Cation influence in adsorptive propane/propylene separation in ZIF-8 (SOD) topology

Andres-Garcia, Eduardo; López-Cabrelles, Javier; Oar-Arteta, Lide; Roldan-Martinez, Beatriz; Cano-Padilla, Marta; Gascon, Jorge; Mínguez Espallargas, Guillermo; Kapteijn, Freek

Important note
To cite this publication, please use the final published version (if applicable).
Please check the document version above.

Cation influence in Adsorptive Propane/Propylene Separation in ZIF-8 (SOD) topology

Eduardo Andres-Garcia[1]*, Javier López-Cabrelles[2], Lide Oar-Arteta[1], Beatriz Roldan-Martinez[1], Marta Cano-Padilla[1], Jorge Gascon[1,3], Guillermo Mínguez Espallargas[2] and Freek Kapteijn[1]*

[1]Catalysis Engineering, ChemE, TUDelft, Van der Maasweg 9, 2629 HZ, Delft, The Netherlands.

[2]Instituto de Ciencia Molecular (ICMol), Universitat de València, c/ Catedrático José Beltrán, 2, 46980 Paterna, Spain.

[3]King Abdullah University of Science and Technology, KAUST Catalysis Center, Advanced Catalytic Materials. Thuwal 23955-6900, Saudi Arabia.

*f.kapteijn@tudelft.nl, e.andresgarcia-1@tudelft.nl; tel: +31 (0)15-2783516

Separation of propylene/propane is one of the most challenging and energy consuming processes in the chemical industry. Propylene demand is increasing and a 99.5 % purity is required for industrial purposes. Adsorption based solutions are the most promising alternatives to improve the economical/energetic efficiency of the process. Zeolitic Imidazolate Frameworks (ZIFs) combine the desired characteristics from both MOFs and zeolites: tunability and flexibility from metal organic frameworks, and exceptional thermal and chemical stability from zeolites. In order to enlighten the role of the cation in the sodalite ZIF-8 framework for propane/propylene separation, dynamic breakthrough measurements have been performed over ZIF-8(Zn), ZIF-67 (i.e. ZIF-8(Co)) and MUV-3 (i.e. ZIF-8(Fe)), all isostructural materials based on the same linker (2-methylimidazole). Cation substitution has a remarkable influence in the framework flexibility, and, consequently, in SOD-ZIF selectivity for light hydrocarbons. The differences between the crystallographic pore sizes of the material and the molecular dimensions of propane and propylene are so small, that the slightest change in the framework causes notable advantages/disadvantages in the final application. While cobalt is known to promote a more rigid framework resulting in an adsorption selectivity towards propane, iron presents the inverse effect yielding selectivity to propylene. Zinc has an intermediate effect. A threshold pressure in the isotherm is observed for propylene uptake by ZIF-67 at 273 and 298 K, and only

at the lower temperature for ZIF-8. Inlet mixture composition does not highly influence the adsorptive selectivity, although it clearly affects the pure hydrocarbon recovery. Over ZIF-67 breakthrough experiments at 298 K yield a temporary pure propylene flow representing 10-15% of the amount fed. ZIF-67 is a promising candidate for propylene/propane adsorptive separation.

1. Introduction

Propylene is one of the most important feedstocks in chemical industry with many applications such as refinery or polymers production. The majority of the propylene (about 64%) [1] is used as feedstock monomer for polypropylene (PP); for which a 99.5 mol% purity is required [2]. Propylene demand has been increasing in the last 10 years, and it is forecast to further globally grow [1, 3]. Despite its importance, propylene is mainly produced as a by-product from ethylene production by steam cracking and in some other refinery processes such as dehydrogenation of paraffins [2, 4]. It is usually obtained as an approximately equimolar mixture of propylene and propane – the alkane can be used for industrial and domestic heating. Nowadays, more on-purpose propylene processes are being developed to cover the current demand gap. Propylene/propane separation is next to ethylene/ethane separation worldwide known as one of the most challenging process in chemical industry [5].

Separation operations have always played a major role in the chemical industry. Not only because they are crucial for production, but also for economic reasons (as investment and energy consumption). Separation processes involve 40-70% of the energy costs of a common chemical plant and up to 10-15% of the world's energy consumption [6, 7]. Similarities in hydrocarbons, both affinities and physical properties (such as volatility and size), lead to the high-energy-consuming distillation. Finding less energy intensive alternatives to these traditional separation techniques means looking

to more tuneable procedures, such as selective adsorption processes, where the chemical properties and framework characteristics of the sorbent materials can make a difference [8].

Adsorption processes stand out as an economical alternative to distillation, as temperature and pressure conditions are less energy intensive and no solvents recoveries are needed [9]. Adsorption consists on the adhesion of molecules from a gas or liquid to the surface of a solid material [10, 11], and adsorptive separation can be ruled by thermodynamics or kinetics, or, most probable, a combination of them: different affinities between adsorbent and adsorbates promote a dominant role of thermodynamics, while kinetics takes the lead when diffusion differences start controlling; steric effects are the more extreme interpretation of kinetics, they are directly related with sizes and shapes of both pores and adsorbed molecules, strongly affecting transport [12]. Industrially, adsorption appears in PSA (or TSA) installations; where several adsorption/desorption columns operate to provide a *quasi*-continuous enriched flow from gas mixtures [7, 11-14]. The characteristics of the adsorbent will determine their suitability for each separation process: BET area, adsorption working capacity, thermal/chemical stability, pore size and structure.

ZIFs (Zeolitic Imidazolate Frameworks) belong to the group of MOFs (Metal-Organic Frameworks) resembling structures of the zeolite family due to the similar bond angle of the imidazole linker and the O-Si-O angle [15]. They combine the advantages of both zeolites (stability) and MOFs (tunability), resulting in new promising crystalline adsorption materials [16-20]. The organic linker is always based on imidazole rings, and its rotation is the cause of the characteristic flexibility of some of their frameworks [21-28]. Functional groups on the imidazole ring may result in different structures or different (non-centro/centro) symmetry in the structure [29]. Their gate opening effect caused by this flexibility is the responsible for the multistage isotherms, and opens a vast spectrum of new possibilities in the adsorptive separation field [12, 15, 27, 30-35]. Some adsorbents have already shown potential in separation processes, and some of them even present the desired inversed selectivity, as ZIF-4 and ZIF-7, with energy savings up to 40% [36, 37]. However, ZIF-4 experiments were performed in conditions with very low inlet flows and large sorbent amounts and ad-

vantageous inlet compositions [38]. ZIF-7 exhibited different threshold pressures for light alkanes and alkenes in their isotherms, yielding a kinetic separation with inverse selectivity of ethane/ethylene mixtures, while for propane/propylene mixtures transport limitations interfered [20, 39, 40]. Not only ZIFs exhibit isotherms with threshold pressures: as an example, MOF NJU-Bai8 also presents a gate opening effect, induced by threshold pressures for propane and propylene; however, this material displays the usual uptake selectivity for propylene[41].

The zinc based ZIF-8 is one of most studied ZIFs in both catalysis and adsorption. It possesses a sodalite structure with a crystallographic pore size of 3.4 Å. Its reported flexibility displays the key of a changing selectivity between alkanes and alkenes [42-44]. ZIF-8 has also been reported to have two symmetries, what could explain this changing behaviour [29]. ZIF-67 is isostructural to ZIF-8, but based on cobalt, with a pore size of 3.3 Å, slightly smaller than ZIF-8 pores. The stiffer Co-N bonds promote a more rigid structure, modifying the effective pore diameter; consequently, ZIF-67 shows inverse selectivity (alkane over alkene) [45-48]. MUV-3, the iron analogue of ZIF-8, has recently been reported, with a pore size of 3.3 Å that resembles ZIF-67 [49]. MUV-3, together with ZIF-8 and ZIF-67, form a perfect triumvirate of microporous materials for a comparative study of the cation influence on framework flexibility and adsorptive alkene/alkane separation. Here, their behaviour in the propylene/propane separation is presented and interpreted.

2. Materials and method

2.1. Sample preparation

ZIF-8 was synthesized according to the procedure reported by Cravillon *et al*, with minor modifications: 2.93 g zinc nitrate hexahydrate ($Zn(NO_3)_2 \cdot 6H_2O$) was dissolved in 200 mL methanol and added to a solution of 6.498 g 2- methylimidazole (Hmim) in 200 mL methanol. The resulting mixture was stirred for 6 hours at room temperature, and the resulting precipitate was filtered and washed with fresh methanol. The final product was dried under vacuum at 353 K, overnight [50].

ZIF-67 was also synthesized according to Cravillon *et al.* In this case, 2.93 g cobalt nitrate hexahy-

drate ($Co(NO_3)_2 \cdot 6H_2O$) were dissolved in 200 mL methanol and mixed with 6.49 g 2-methylimidazole (Hmim), also in 200 mL methanol. After stirring the solution for 8 h. at room temperature, it was filtered. The purple precipitate was collected, washed with fresh methanol and also dried under vacuum at 353 K, overnight.

MUV-3 was synthesized following the reported procedure by Lopez-Cabrelles *et al.* [49]. This ZIF, based on Fe^{2+}, is sensitive to air and moisture exposure. Therefore, this material was handled and transferred into a column in a glove box.

2.2. Sample characterization

The XRD patterns from ZIF-8 and ZIF-67 powders were recorded in Bragg–Brentano geometry with a Bruker D8 Advance X-ray diffractometer equipped with a LynxEye position sensitive detector. Measurements were performed at room temperature, by using monochromatic Co $K\alpha$ (λ= 1.788970 Å) radiation between 2θ= 5° and 50°. MUV-3 was measured using monochromatic Cu $K\alpha$ ($\lambda = 1.5406$ Å), and the data were converted afterwards to be presented with ZIF-8 and ZIF-67.

Thermogravimetric Analysis (TGA) was performed on a Mettler Toledo TGA/SDTA1 with a sample robot (TSO 801RO) and gas control (TSO 800GC1). The method consisted in a temperature range from 303 to 1073 K, at a heating rate of 5 K min^{-1}, under air flow (100 cm_{STP}^3 min^{-1}).

Textural properties of sodalite ZIFs were analysed by N_2 adsorption/desorption at 77 K and by propane/propylene measurements at 273 K and 298 K. Gas adsorption isotherms were measured by a volumetric method, in a Tristar II 3020 Micromeritics instrument. All samples were outgassed before the measurement at 353 K overnight.

2.3. Dynamic adsorption measurements

The Breakthrough set-up is based on a packed adsorption column with pressure/temperature control and continuous analysis of the outlet flow upon step changes in feed composition. A small hydrogen flow is added as a nonadsorbing tracer. The lay-out of the set-up is such that this results in determination of the outlet flow rates of the individual components Two analysis instruments are available: i) a Mass Spectrometer (MS) and ii) a Compact Gas Chromatograph (CGC). Due to the

overlapping fragmentation patterns from propane and propylene in the MS, for propane m/e 29 and for propylene m/e 40 were taken as characteristic m/e intensities. To increase time resolution of the quantitative CGC analysis, the equipment is equipped with three parallel capillary columns, connected to three Flame Ionization Detectors (FID), allowing a *quasi*-continuous analysis (every 20 s). For the following dynamic experiments, 1.6 g ZIF-8 and 1.5 g ZIF-67 (both pelletized at 4 ton/m^2 and sieved to 500-1000 μm)) and 1.8 g MUV-3 (not needed to be pelletized due to the size of MUV-3 crystals, 300 μm) were used. These materials were tested at 298 K and a pressure of 2 bara (absolute pressure). As propane/propylene separation is extremely energy demanding, energy-saving temperature/pressure conditions were chosen to increase the efficiency of the process. The equimolar propane/propylene mixture (actual refinery compositions) [51] was fed as follows: 3.5 ml min^{-1} of both components and 1 ml min^{-1} H$_2$ as non-adsorbing tracer. For the non-equimolar mixtures, the inlet flows are used as follows: i) 3.5 ml min^{-1} propylene, 0.5 ml min^{-1} propane and 1 ml min^{-1} H$_2$ (alkene-rich), ii) 3.5 ml min^{-1} propane, 0.5 ml min^{-1} propylene and 1 ml min^{-1} H$_2$ (alkane-rich). Each adsorbent was regenerated after every experiment in 10 ml min^{-1} He flow at 2 bara for 2 h at 298 K. In the presented breakthrough graphs time zero is set with the first MS detection of hydrogen.

3. Results and Discussion

3.1. Sample characterization

XRD patterns from the three zeolitic adsorbents are presented in Figure 1a, together with the simulated pattern of a typical sodalite structure. The resemblance of the reflections confirms the framework of three samples. In the same order, the comparison of the TGA profiles from those ZIFs is displayed in Figure 1b. Thermal stability up to 500 K is observed; however, MUV-3 is the most thermosensitive of the three, being sensitive also to water and oxygen contact.
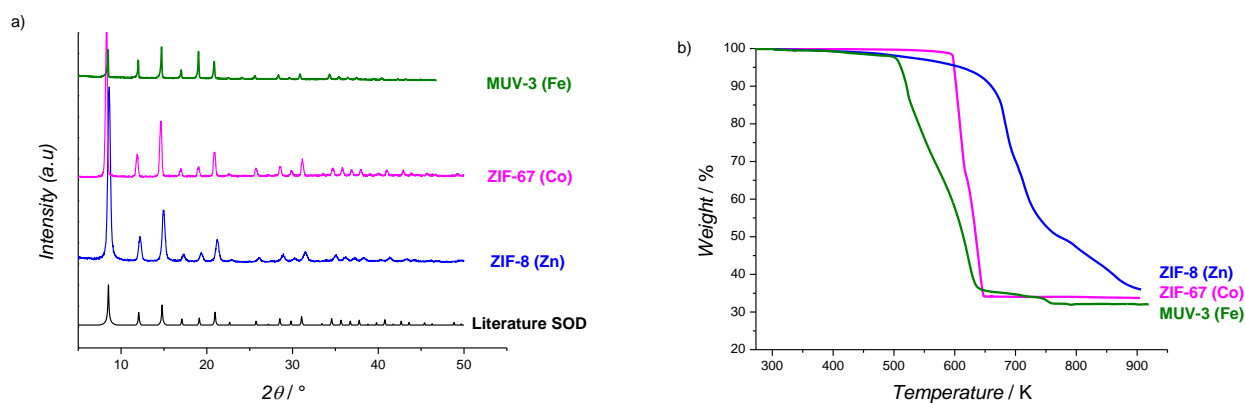
Figure 1. ZIF-SOD characterization by *(a)* XRD (λ =1.788970 Å); and *(b)* TGA in air at 5 K min^{-1}.

Nitrogen adsorption isotherms at 77 K are displayed in Figure 2. Capacities of ZIF-8 and ZIF-67 are similar and significantly higher than of MUV-3, which is easily compared through BET area and microporous volume values: S_{BET}= 1340 m^{2}g^{-1} and $V_{micropore}$= 0.56 cm^{3}g^{-1} for ZIF-8; S_{BET}= 1500 m^{2}g^{-1} and $V_{micropore}$= 0.66 cm^{3}g^{-1} for ZIF-67; and S_{BET}= 450 m^{2}g^{-1} and $V_{micropore}$= 0.20 cm^{3}g^{-1} for MUV-3. This BET area of MUV-3 is lower than the previously reported value of 960 m^{2}g^{-1} [49], and is attributed to the presence of residual template molecules, required in its synthesis, which are very difficult to be removed. However, the most interesting are the differences in adsorption steps attributed to the framework flexibility. Next to the low-pressure uptake step, ZIF-8 presents one extra step in the adsorption branch of the isotherm, ZIF-67 shows two extra steps, and MUV-3 none, as the close-ups of Figure 2 display (isotherm Type I). The step in the ZIF-8 isotherm is attributed to the adsorption induced change in its symmetry by the linker movement. By analogy the more rigid ZIF-67 (reduced oscillatory motion), displaying even two steps, is suggested to undergo even two changes [44, 46, 52]. A less rigid one metal ion-N bond in MUV-3(Fe) would explain the difficulty to observe the remarkable opening step from the other ZIFs (as). This is a nice demonstration of the influence of framework flexibility due to cation substitution in sodalite ZIF's. It is therefore anticipated that adsorption properties will be affected by the small differences in the sodalite framework of these materials.
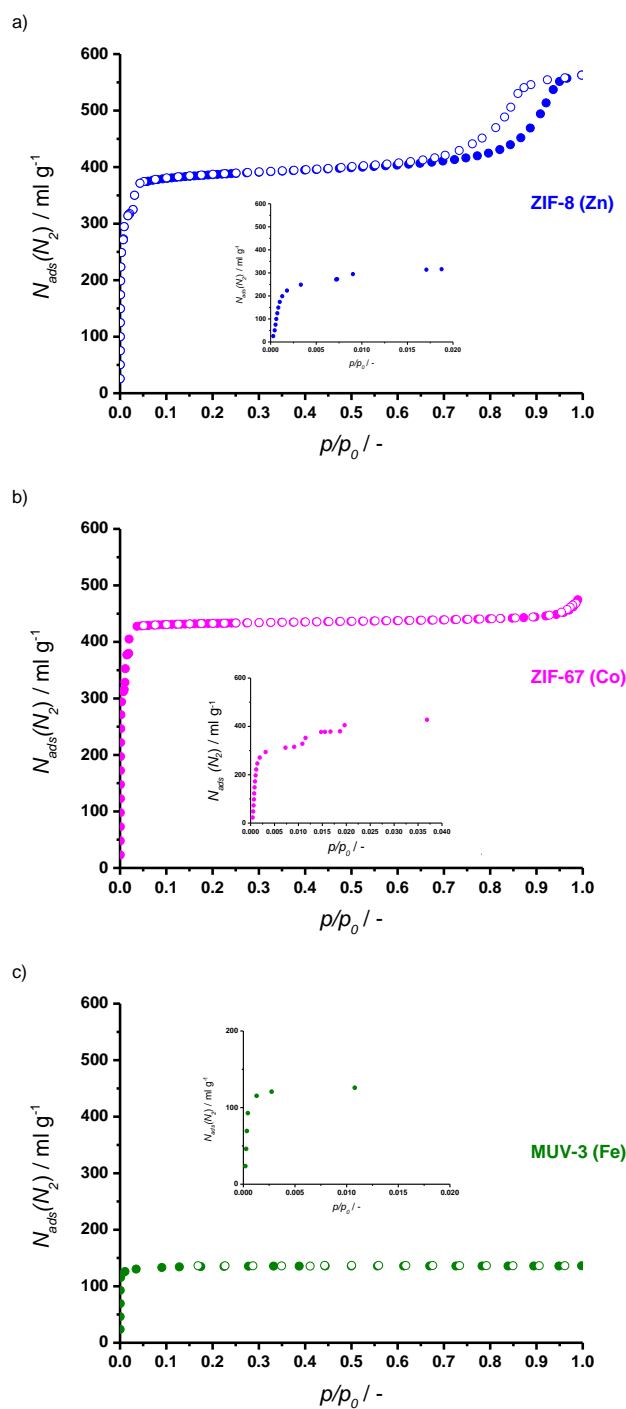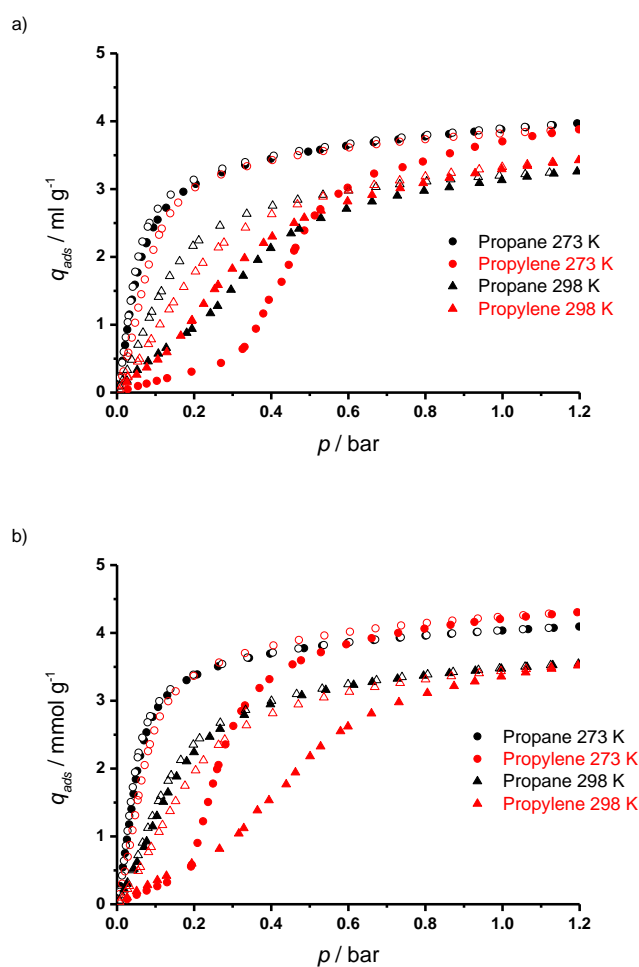
Figure 2. Low pressure adsorption/desorption isotherms (volumetric measurement) for nitrogen at 77 K, on: *(a)* ZIF-8, *(b)* ZIF-67, and *(c)* MUV-3. Solid symbols for adsorption and open ones for desorption.

Adsorption isotherms of propane and propene at 273 K and 298 K were determined for a better understanding of the flexibility influence (Figure 3). For all three ZIFs, the 273 K capacities exceed those at 298 K, as thermodynamically expected. However, the most interesting aspect of these profiles is what happens at lower pressures. Even if both propylene and propane present similar uptakes

at 1 bar, they substantially differ below 0.5 bar. Once again, the cation has an influence on that difference: *i*) ZIF-8 (Figure 3a) shows a threshold pressure in the propylene adsorption branch at 273 K, but this effect disappears at 298 K, where the adsorption and desorption profiles concur for both hydrocarbons; *ii*) ZIF-67 (Figure 3b) displays a threshold pressure at both temperatures; and *iii*) MUV-3 (Figure 3c) shows lower uptakes, but behaves similar as ZIF-8: a threshold at low pressure at 273 K and a slightly higher uptake of propylene than propane at 1 bar and 298 K. The MUV-3 capacities at 1 bar correspond with the N_2 uptakes (Figure 2c).
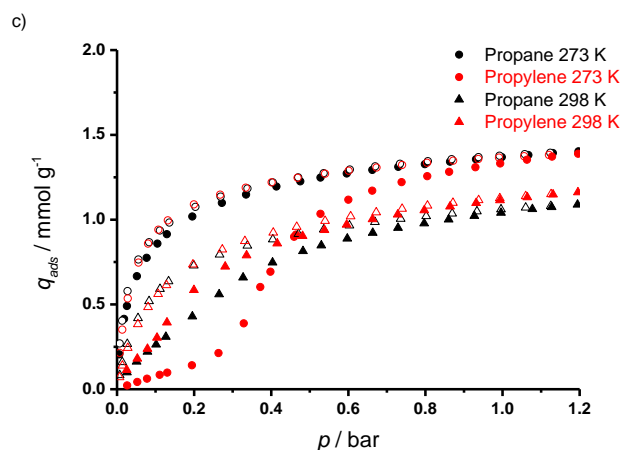
a)

b)

Figure 3. Low pressure adsorption/desorption isotherms (volumetric measurement) for propane (*black*) and propylene (*red*) at 273 K (*spheres*) and 298 K (*triangles*), on: *(a)* ZIF-8, *(b)* ZIF-67, and *(c)* MUV-3. Solid symbols for adsorption and open ones for desorption.

As noted for the nitrogen adsorption, the substituting cation (Zn, Co and Fe) modifies the flexibility of the framework, and its effect in hydrocarbons diffusion is clearly observed in their adsorption isotherms at different temperatures. At 273 K, all materials show a delay in the propylene uptake. Only ZIF-67 exhibits this effect at higher temperature. This is in line with the observations that at higher temperatures the threshold pressure usually shifts to higher values or disappears [40, 41].

In view of the 'normal' desorption profile in these cases and the coincidence of the adsorption and desorption profiles at 298 K for ZIF-8 and MUV-3, the observed threshold pressure is attributed to a kinetic phenomenon. The equilibrium stabilization times around this threshold pressure in the iso-therm measurements were also much larger than in the absence of this effect (see Supplementary Material), supporting this conclusion. The subtle differences between these ZIF samples are most visible at 298 K, therefore breakthrough experiments have been conducted at 298 K.

3.2. Dynamic adsorption measurements

Figures 4, 5 and 6 shows breakthrough profiles, performed at 298 K and 2 bara, for ZIF-8, ZIF-67 and MUV-3; zero time on stream is set with the first H_2 detection. GC analysis complements MS results, and both curves are displayed together for a complete analysis. The equimolar hydrocarbons

feed flow results are summarized in Figure 4 and Table 1. Table 1 contains a*dsorbed amounts* of both hydrocarbons, *adsorption selectivity* (AS; eq. 1), *pure product* (PP; eq. 2) and *recovery ratio* (RR; eq. 3) values. AS evaluates the amounts adsorbed and accounts for the inlet flow composition (equimolar for these first experiments). PP represents the amount recovered of one the hydrocarbons (propylene for ZIF-8 and ZIF-67; propane for MUV-3, shaded in green) when this elutes pure from the column. PP area is defined in the Supplementary Material (Figure SM.1). RR shows percentage recovered pure of one of the hydrocarbons, relative to its total amount fed. RR is evaluated until the breakthrough of the second hydrocarbon (propane for ZIF-8 and ZIF-67; propylene for MUV-3, shaded in green in Table 1).

$$\text{Adsorption Selectivity (AS)} = \frac{q_{ads}(C_3)/F_0(C_3)}{q_{ads}(C_3^=)/F_0(C_3^=)} \quad ; \quad \text{(eq. 1)}$$

$$\text{Pure Product (PP)} = \frac{q_{pureHC1}}{weight_{ZIF}} \quad ; \quad \text{(eq. 2)}$$

$$\text{Recovery Ratio (RR)} = \frac{q_{pureHC1}}{q_{fed,HC1}} * 100 \quad ; \quad \text{(eq. 3)}$$
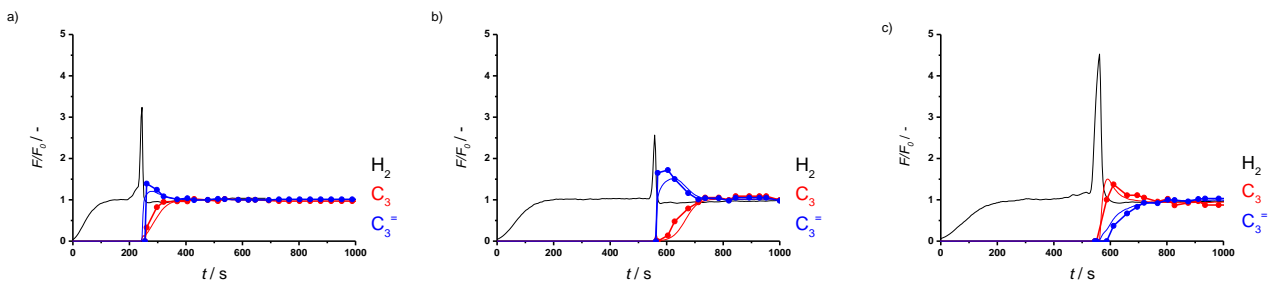
Figure 4. Breakthrough normalized exit flowrates vs time for equimolar propane/propylene feed (C_3:$C_3^=$:H_2 = 3.5:3.5:1) at 298 K and 2 bara on *(a)* ZIF-8, *(b)* ZIF-67, and *(c)* MUV-3. CGC analysis (lines and symbols) over MS analysis (lines).

Table 1. Adsorbed amounts, AS, PP and RR, determined from breakthrough profiles for equimolar propane/propylene feed (C_3:$C_3^=$:H_2 = 3.5:3.5:1) at 298 K and 2 bara on *(top)* ZIF-8, *(centre)* ZIF-67, and *(bottom)* MUV-3. (CGC analysis).

3.5:3.5 ; C_3:$C_3^=$				
q_{ads} C_3 $(mmol\ g^{-1})$	q_{ads} $C_3^=$ $(mmol\ g^{-1})$	AS -	PP $(mmol\ g^{-1})$	RR %
ZIF-8 0.50	0.41	1.20	0.05	7.4
ZIF-67 1.10	0.88	1.25	0.19	12.2
MUV-3 0.77	0.91	0.85	0.08	4.9

Hydrogen, as tracer, is the first gas to break through the column, while both hydrocarbons are still being adsorbed. When the first hydrocarbon breaks through, a sharp hydrogen peak is observed, as the consequence of gas accumulation in the downstream lines; it is just an artefact of the setup to determine flow rates of components leaving the column [45]. Before the second hydrocarbon also breaks through, a roll-up phenomenon is observed in the breakthrough of the first component, attributed to a displacement from the sodalite framework of the first by the second component. Contrary to what is usually observed for most adsorbents, propylene is the first gas to break through in case of ZIF-8, and much more pronounced in case of ZIF-67, providing temporarily a highly alkene enriched flow, required in polymer industry [45]. Regeneration was performed at mild conditions (10 ml min^{-1} He flow, at 2 bara and 298 K, for 2 h) and the samples were used throughout the whole series of experiments; Figure SM.3 and Table SM.3 provide an example of reproducibility on ZIF-67. Figure SM.2 shows absolute exit flowrates and composition from a repeated breakthrough experiment as presented in Fig. 4.b.

The most remarkable observation in Figure 4 is the changing selectivity among the sodalite ZIFs. As adsorption isotherms already showed (Figure 3), these materials behave in a different manner at 298 K depending on the cation in their framework. ZIF-67 showed a marked threshold pressure in the propylene adsorption isotherm, and consequently an inverse adsorption selectivity (towards propane) is observed in the breakthrough profiles. MUV-3 – without threshold pressure at 298 K and higher propylene than propane capacity – obviously displays the more common selectivity to the alkene, providing separation between hydrocarbons but retaining the desired propylene, thus an ef-

ficient recovery step must be incorporated to obtain this component pure [9]. ZIF-8, the most common of the ZIFs family, appears to exhibit an intermediate behaviour between the previous two structures, and no good separation is obtained. Thus, ZIF-67 is the one standing out by its separation parameters (Table 1).

Figures 5 and 6 and Table 2 collect the results from the breakthrough experiments, also at 298 K and 2 bara, for ZIF-8, ZIF-67 and MUV-3 using excess of one of the components in order to study the effect of the alkane/alkene inlet feed ratio. Table 2 contains adsorbed amounts of both hydrocarbons, and the AS, PP and RR parameters.

Figure 5. Breakthrough normalized exit flowrates vs time for propane rich feed ($C_3:C_3^=:H_2 = 3.5:0.5:1$) at 298 K and 2 bara on *(a)* ZIF-8, *(b)* ZIF-67, and *(c)* MUV-3. CGC analysis (lines, symbols) over MS analysis (lines).
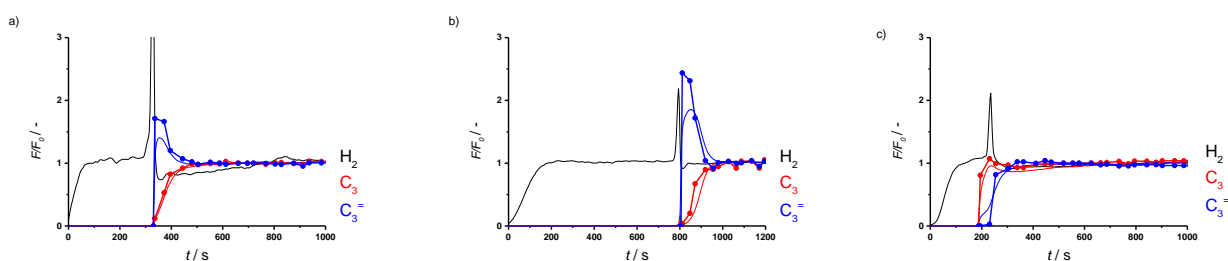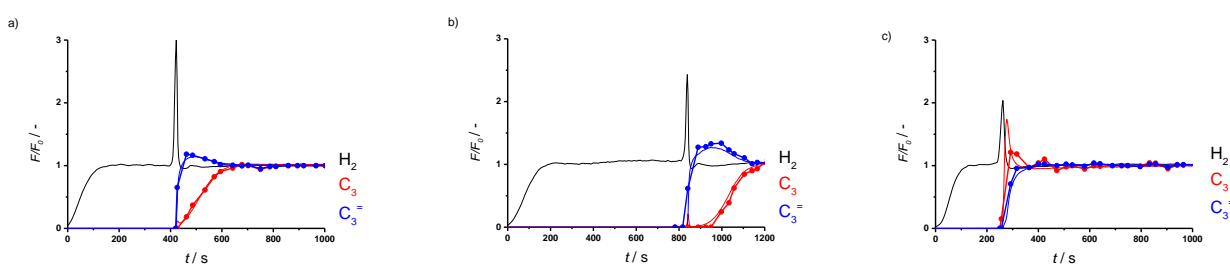

Figure 6. Breakthrough normalized exit flowrates vs time for propylene rich feed ($C_3:C_3^=:H_2 = 0.5:3.5:1$) at 298 K and 2 bara on *(a)* ZIF-8, *(b)* ZIF-67, and *(c)* MUV-3. CGC analysis (lines, symbols) over MS analysis (lines).

Table 2. Adsorbed amounts, AS, PP and RR, determined from breakthrough profiles for non-equimolar hydrocarbons mixtures: $C_3:C_3^=:H_2$ (3.5:0.5:1 and 0.5:3.5:1, *left* and *right*, respectively) at 298 K and 2 bara on *(top)* ZIF-8, *(centre)* ZIF-67, and *(bottom)* MUV-3 (CGC analysis).

3.5:0.5 ; $C_3:C_3^=$					
	q_{ads} C_3 (mmol g^{-1})	q_{ads} $C_3^=$ (mmol g^{-1})	AS -	PP (mmol g^{-1})	RR %
ZIF-8	0.67	0.07	1.31	0.01	9.7
ZIF-67	1.56	0.18	1.23	0.03	9.2
MUV-3	0.40	0.07	0.86	0.10	14.3

0.5:3.5 ; $C_3:C_3^=$					
	q_{ads} C_3 (mmol g^{-1})	q_{ads} $C_3^=$ (mmol g^{-1})	AS -	PP (mmol g^{-1})	RR %
ZIF-8	0.13	0.75	1.25	0.07	6.1
ZIF-67	0.27	1.39	1.35	0.35	13.8
MUV-3	0.06	0.47	0.89	0.00	0.4

Figure 5 shows results for a propane-rich inlet flow, while Figure 6 presents that for a propylene-rich inlet flow. As MUV-3 displays opposite selectivity than ZIF-8 and ZIF-67, results will be compared for Figure 5a, 5b and 6c (high inlet concentration of the selectively adsorbed hydrocarbon), and for Figure 6a, 6b and 5c (high inlet concentration of the non-selectively adsorbed hydrocarbon). In the first situation, the higher concentration of the selectively-adsorbed-hydrocarbon in the feed flow (propane for ZIF-8 and ZIF-67, propylene for MUV-3) promotes *i*) a sharper higher elution peak of the first hydrocarbon, and *ii*) smaller normalised area between both hydrocarbon breakthrough profiles, and so, a lower PP. The higher concentration of the preferentially adsorbed hydrocarbon quickly saturates the framework, reducing the separation, resulting in just some displacement in breakthrough time of one compared to the other component. AS is not remarkably affected by the applied compositions, and both PP and RR decrease (with the exception of ZIF-8 RR, where an earlier saturation decreases the fed hydrocarbon).

For the second situation, the hydrocarbon with the lower concentration is now selectively adsorbed, thus: *i*) the sharp elution peak of the first hydrocarbon that breaks through has almost disappeared, as sorbate displacement is considerably reduced, and *ii*) the time difference (and integrated area) between the hydrocarbon profiles increases, and so the PP. As the flow rate of the second hydrocar-

bon is considerably lower, time to saturation is larger; the long time needed to completely saturate the ZIF, promotes an enriched outlet flow for the first hydrocarbon to break through. By contrast with the previous inlet composition, PP and RR increase (with the same ZIF-8 exception). In practice this inlet feed composition is not frequently encountered, thus, this separation would ideally only be performed as a second step in an industrial process after an equimolar inlet separation step, where the enriched outlet will become the inlet of a purification step, in order to reach required subsequent final specifications. Debottlenecking a distillation process could also be a potential purpose for this separation condition.

A first important observation is the difference noted between the adsorbed amounts in the isotherms (static measurements) and breakthrough experiments (dynamic measurements). While both ZIF-8 and ZIF-67 exhibit a much lower uptake than expected (especially ZIF-8 reaches only about 40% of the equilibrium isotherm value), the MUV-3 uptake is in line with the isotherm levels. Tables SM.1-2 in Supplementary Material show the elapsed equilibration times of the hydrocarbons isotherm measurements, what helps to understand this behaviour. Equilibration times for ZIF-8 are much longer than for MUV-3, the uptake of propane in ZIF-67 is much faster than of propylene (the slowest of all), all indicative of the interference of kinetics. This much lower uptake in the breakthrough than in the isotherm measurements was also observed in literature, for example, for hydrocarbons adsorption in ZIF-4 [38, 43]. These observations support the interpretation of a kinetically controlled uptake/breakthrough process. ZIF-67 had the highest micropore volume (Fig. 2.b, nitrogen isotherm), thus, even with the reduced dynamic uptake, the large amount of adsorbed propane is remarkable. Its values in the separation parameters and its inverse selectivity extol its potential in this challenging separation.

Secondly, a kinetic selectivity is often explained on the basis of pore and sorbate dimensions. However, the three ZIFs present quite similar pore sizes 3.3-3.4 Å [15, 46, 49] and there is no clear picture which sorbate dimensions to consider. Propylene's '*kinetic diameter*' is larger than the one of propane (0.45 nm against 0.43 nm), but on the other hand, propylene '*Van der Waals diameter*' and

'*critical molecular diameter*' show the opposite relationship (0.40 nm and 0.27 nm for propylene, versus 0.42 nm and 0.28 nm for propane; respectively) [42, 53, 54]. Thus, the concept of "diffusional hierarchy" is not so evident, as the shape of the molecules is another parameter to consider, next to affinities, and of course the special characteristics of the selected microporous sorbent. Also for a zeolite as DD3R these shape parameters play a decisive role in the adsorptive separation of C_3 and C_4 hydrocarbons mixtures [19, 55]. The exact mechanism of adsorbing propane and rejecting propylene, like suggested for ZIF-7 [40], is not yet fully clarified for these ZIFs, but pore size and framework flexibility play a dominant role. Structural flexibility in the sodalite framework has already been studied [22, 35]. This property has a great impact on the diffusivity of the studied gases, controlling the selectivity of the ZIFs depending on the metal cation [46]. The methyl rotation potential is altered in ZIF-67 framework (from its isostructural ZIF-8), as its crystal structure is slightly more contracted due to the cobalt-N bond [56].

ZIF-67 and MUV-3 display a clear dependence on inlet flow composition, and are the extremes of this triumvirate of materials. Both adsorbents provide temporary pure single hydrocarbon flows (PP), which represents an important fact for industrial applications. ZIF-8 presents intermediate results, as it only shows enrichment, and not a pure component flow. The observed dynamic selectivity AS is barely feed-composition dependent (Tables 1 and 2). The specific amounts of pure product PP remarkably increases when the inlet is enriched to the non-selectively adsorbed component. The corresponding fraction pure component recovered RR amount to 5-10 % for ZIF-8, 10-15 % for ZIF-67 and 0-15 % for MUV-3, being the iron substituted ZIF the most influenced by the inlet mixture composition. By comparison with literature, ZIF-67 presents the highest pure fraction recoveries at high flows/adsorbent content ratio and with 1:1 propane-propylene feed mixture [38].

The difference in the selectivity is explained through the three existing separation mechanisms: *i) thermodynamic control*: equilibrium adsorption dominated mostly by adsorption enthalpies and entropies; *ii) kinetics control*: dominance of diffusion, and, sometimes, gate-opening effects; *iii) molecular sieving*: limiting situation of kinetics, where some molecules fit in the pores and other are

excluded, as recently has been reported for ethane/ethene mixture over another MOF ($Fe_2(O_2)$dobc) [39]. ZIF-67 stands out its competitors for the adsorptive separation of propane/propylene mixtures; the rigidity of its framework promotes kinetics to a dominant role (*mechanism ii*), resulting in an inverse selectivity. The effluent is enriched in propylene, in agreement with the clear threshold adsorption pressure present in Figure 3b, and an observation attractive for its industrial application. On the other hand a high pressure decreases this kinetics controlled effect [45] as both components are forced into the framework at higher pressures. Further, only 10-15% of the propene fed is collected in pure form, which may moderate the application potential. Another sorbent, ZIF-7, presented a similar behaviour for ethane/ethene mixtures [20, 40]. In case of ZIF-8 *mechanism ii* is less prominent, and clearly influenced by temperature [43, 44]. Separation by MUV-3, with a predicted less rigid framework, is consequently ruled by thermodynamics, and π-bond interaction of the alkene with the Fe^{2+} cation is expected to be responsible for the propylene adsorption selectivity (*mechanism i*).

4. Conclusions

Three isostructural ZIFs (SOD framework with Zn, Co or Fe) are characterized and compared for their performance in the adsorptive separation of propane-propylene mixtures.

Static adsorption measurements show a remarkable threshold pressure in propylene adsorption at 273 K for all samples, but only ZIF-67 keeps its remarkable behaviour at higher temperature (298 K, more energy efficient conditions), placing it as the most promising sorbent candidate in propylene/propane separation. BET area and micropore volume of ZIF-67 are the largest, followed by ZIF-8. MUV-3 presents the lowest capacity of the trio.

Dynamic adsorption measurements (breakthrough experiments) display selectivity changes with metal cation substitution: while MUV-3 presents the common adsorption preference for the alkene, ZIF-67 exhibits an inverse selectivity: adsorbing the alkane and providing a purified propylene flow. The ZIF-8 inverse selectivity is less pronounced, as it can even be tuned with synthe-

sis/temperature/pressure conditions (based on previous publications). Cobalt is known to promote a more rigid sodalite framework; the small changes in the pore size, by the gate-opening effect, are enough to inverse the selectivity of ZIF-67: the separation is now ruled by a kinetic mechanism. Iron, on the other hand, is expected to increase the flexibility on the MOF; as a result, thermodynamics dominate the process on MUV-3. ZIF-8, with zinc, has an intermediate behaviour. Propylene is, as a rule, thermodynamically preferentially adsorbed over propane, but kinetics and diffusion can be controlled by the framework flexibility.

Breakthrough analysis also shows that kinetically controlled processes promote lower than equilibrium adsorbed amounts of hydrocarbons. Feed composition affect the recovery of the pure product. Reducing the concentration of the selectively adsorbed hydrocarbon promotes an improvement in separation efficiency, for ZIF-67 up to 15% of propylene is obtained as pure product.

Hydrocarbons adsorptive selectivity on ZIF-SOD is controlled by the sodalite framework rigidity, and can be tuned by cation substitution. ZIF-67 stands out in this ZIFs group for propylene/propane separation.

Acknowledgements

References

[1] J.S. Plotkin, The changing dynamics of olefin supply/demand, Catalysis Today, 106 (2005) 10-14.

[2] H. Jarvelin, J.R. Fair, Adsorptive separation of propylene-propane mixtures, Industrial & Engineering Chemistry Research, 32 (1993) 2201-2207.

[3] I. Markit, Propylene. Chemical Economics Handbook, IHS Markit, 2017.

[4] T. Ren, M. Patel, K. Blok, Olefins from conventional and heavy feedstocks: Energy use in steam cracking and alternative processes, Energy, 31 (2006) 425-451.

[5] A. van Miltenburg, J. Gascon, W. Zhu, F. Kapteijn, J. Moulijn, Propylene/propane mixture adsorption on faujasite sorbents, Adsorption, 14 (2008) 309-321.

[6] D.S. Sholl, R.P. Lively, Seven chemical separations to change the world, Nature 532 (2016) 435–437.

[7] P.C. Wankat, Separation Process Engineering: includes mass transfer analysis. (4th ed.), Prentice Hall, Massachusetts (USA), 2017.

[8] O.R.N.L. (ORNL), Materials for Separation Technologies. Energy and Emission Reduction Opportunities., Tennessee (USA), 2005.

[9] C.A. Grande, A.E. Rodrigues, Propane/Propylene Separation by Pressure Swing Adsorption Using Zeolite 4A, Industrial & Engineering Chemistry Research, 44 (2005) 8815-8829.

[10] C.A. Grande, Advances in Pressure Swing Adsorption for Gas Separation, ISRN Chemical Engineering, 2012 (2012) 13.

[11] D.M. Ruthven, Principles of Adsorption and Adsorption Processes, John Wiley & Sons, 1984.

[12] R.T.e. Yang, Adsorbent - Fundamentals and Applications, Wiley Inter-Science, 2003.

[13] S. Sircar, T.C. Golden, M.B. Rao, Activated carbon for gas separation and storage, Carbon, 34 (1996) 1-12.

[14] J.U.S. Keller, R., Gas Adsorption Equilibria: Experimental Methods and Adsorptive Isotherms, Springer, New York (USA), 2005.

[15] K.S. Park, Z. Ni, A.P. Côté, J.Y. Choi, R. Huang, F.J. Uribe-Romo, H.K. Chae, M. O'Keeffe, O.M. Yaghi, Exceptional chemical and thermal stability of zeolitic imidazolate frameworks, Proceedings of the National Academy of Sciences, 103 (2006) 10186-10191.

[16] Y. Wu, H. Chen, D. Liu, Y. Qian, H. Xi, Adsorption and separation of ethane/ethylene on ZIFs with various topologies: Combining GCMC simulation with the ideal adsorbed solution theory (IAST), Chemical Engineering Science, 124 (2015) 144-153.

[17] N. Hara, M. Yoshimune, H. Negishi, K. Haraya, S. Hara, T. Yamaguchi, Diffusive separation of propylene/propane with ZIF-8 membranes, Journal of Membrane Science, 450 (2014) 215-223.

[18] T. Wu, X. Bu, J. Zhang, P. Feng, New Zeolitic Imidazolate Frameworks: From Unprecedented Assembly of Cubic Clusters to Ordered Cooperative Organization of Complementary Ligands, Chemistry of Materials, 20 (2008) 7377-7382.

[19] W. Zhu, F. Kapteijn, J.A. Moulijn, J.C. Jansen, Selective adsorption of unsaturated linear C4 molecules on the all-silica DD3R, Physical Chemistry Chemical Physics, 2 (2000) 1773-1779.

[20] C. Gücüyener, J. van den Bergh, J. Gascon, F. Kapteijn, Ethane/Ethene Separation Turned on Its Head: Selective Ethane Adsorption on the Metal−Organic Framework ZIF-7 through a Gate-Opening Mechanism, Journal of the American Chemical Society, 132 (2010) 17704-17706.

[21] W. Morris, C.J. Stevens, R.E. Taylor, C. Dybowski, O.M. Yaghi, M.A. Garcia-Garibay, NMR and X-ray Study Revealing the Rigidity of Zeolitic Imidazolate Frameworks, The Journal of Physical Chemistry C, 116 (2012) 13307-13312.

[22] D. Fairen-Jimenez, S.A. Moggach, M.T. Wharmby, P.A. Wright, S. Parsons, T. Düren, Opening the Gate: Framework Flexibility in ZIF-8 Explored by Experiments and Simulations, Journal of the American Chemical Society, 133 (2011) 8900-8902.

[23] H.-C. Zhou, J.R. Long, O.M. Yaghi, Introduction to Metal−Organic Frameworks, Chemical Reviews, 112 (2012) 673-674.

[24] W. Morris, B. Leung, H. Furukawa, O.K. Yaghi, N. He, H. Hayashi, Y. Houndonougbo, M. Asta, B.B. Laird, O.M. Yaghi, A Combined Experimental−Computational Investigation of Carbon

Dioxide Capture in a Series of Isoreticular Zeolitic Imidazolate Frameworks, Journal of the American Chemical Society, 132 (2010) 11006-11008.

[25] S. Aguado, G. Bergeret, M.P. Titus, V. Moizan, C. Nieto-Draghi, N. Bats, D. Farrusseng, Guest-induced gate-opening of a zeolite imidazolate framework, New Journal of Chemistry, 35 (2011) 546-550.

[26] A. Arami-Niya, G. Birkett, Z. Zhu, T.E. Rufford, Gate opening effect of zeolitic imidazolate framework ZIF-7 for adsorption of CH4 and CO2 from N2, Journal of Materials Chemistry A, 5 (2017) 21389-21399.

[27] A. Phan, C.J. Doonan, F.J. Uribe-Romo, C.B. Knobler, M. O'Keeffe, O.M. Yaghi, Synthesis, Structure, and Carbon Dioxide Capture Properties of Zeolitic Imidazolate Frameworks, Accounts of Chemical Research, 43 (2010) 58-67.

[28] A. Gonzalez-Nelson, F.-X. Coudert, M.A. van der Veen, Rotational Dynamics of Linkers in Metal–Organic Frameworks, Nanomaterials, 9 (2019) 330.

[29] S. Van Cleuvenbergen, Z.J. Smith, O. Deschaume, C. Bartic, S. Wachsmann-Hogiu, T. Verbiest, M.A. van der Veen, Morphology and structure of ZIF-8 during crystallisation measured by dynamic angle-resolved second harmonic scattering, Nature Communications, 9 (2018) 3418.

[30] B. Zheng, Y. Pan, Z. Lai, K.-W. Huang, Molecular Dynamics Simulations on Gate Opening in ZIF-8: Identification of Factors for Ethane and Propane Separation, Langmuir, 29 (2013) 8865-8872.

[31] B. Wang, A.P. Cote, H. Furukawa, M. O/'Keeffe, O.M. Yaghi, Colossal cages in zeolitic imidazolate frameworks as selective carbon dioxide reservoirs, Nature, 453 (2008) 207-211.

[32] J. McEwen, J.-D. Hayman, A. Ozgur Yazaydin, A comparative study of CO2, CH4 and N2 adsorption in ZIF-8, Zeolite-13X and BPL activated carbon, Chemical Physics, 412 (2013) 72-76.

[33] L. Hauchhum, P. Mahanta, Carbon dioxide adsorption on zeolites and activated carbon by pressure swing adsorption in a fixed bed, International Journal of Energy and Environmental Engineering, 5 (2014) 349-356.

[34] J. Rouquerol, F. Rouquerol, 3 - Methodology of Gas Adsorption, in: F. Rouquerol, J. Rouquerol, K.S.W. Sing, P. Llewellyn, G. Maurin (Eds.) Adsorption by Powders and Porous Solids (Second Edition), Academic Press, Oxford, 2014, pp. 57-104.

[35] D. Fairen-Jimenez, R. Galvelis, A. Torrisi, A.D. Gellan, M.T. Wharmby, P.A. Wright, C. Mellot-Draznieks, T. Düren, Flexibility and swing effect on the adsorption of energy-related gases on ZIF-8: combined experimental and simulation study, Dalton Transactions, 41 (2012) 10752-10762.

[36] R. van Wissen, M. Golombok, J.J.H. Brouwers, Separation of carbon dioxide and methane in continuous countercurrent gas centrifuges, 2005.

[37] A. Mersmann, B. Fill, R. Hartmann, S. Maurer, The Potential of Energy Saving by Gas-Phase Adsorption Processes, Chemical Engineering & Technology, 23 (2000) 937-944.

[38] M. Hartmann, U. Bohme, M. Hovestadt, C. Paula, Adsorptive Separation of Olefin/Paraffin Mixtures with ZIF-4, Langmuir, 31 (2015) 12382-12389.

[39] L. Li, R.-B. Lin, R. Krishna, H. Li, S. Xiang, H. Wu, J. Li, W. Zhou, B. Chen, Ethane/ethylene separation in a metal-organic framework with iron-peroxo sites, Science, 362 (2018) 443-446.

[40] J. van den Bergh, C. Gücüyener, E.A. Pidko, E.J.M. Hensen, J. Gascon, F. Kapteijn, Understanding the Anomalous Alkane Selectivity of ZIF-7 in the Separation of Light Alkane/Alkene Mixtures, Chemistry – A European Journal, 17 (2011) 8832-8840.

[41] X. Wang, R. Krishna, L. Li, B. Wang, T. He, Y.-Z. Zhang, J.-R. Li, J. Li, Guest-dependent pressure induced gate-opening effect enables effective separation of propene and propane in a flexible MOF, Chemical Engineering Journal, 346 (2018) 489-496.

[42] P. Krokidas, M. Castier, S. Moncho, E. Brothers, I.G. Economou, Molecular Simulation Studies of the Diffusion of Methane, Ethane, Propane, and Propylene in ZIF-8, The Journal of Physical Chemistry C, 119 (2015) 27028-27037.

[43] U. Böhme, B. Barth, C. Paula, A. Kuhnt, W. Schwieger, A. Mundstock, J. Caro, M. Hartmann, Ethene/Ethane and Propene/Propane Separation via the Olefin and Paraffin Selective Metal–Organic Framework Adsorbents CPO-27 and ZIF-8, Langmuir, 29 (2013) 8592-8600.

[44] K. Li, D.H. Olson, J. Seidel, T.J. Emge, H. Gong, H. Zeng, J. Li, Zeolitic Imidazolate Frameworks for Kinetic Separation of Propane and Propene, Journal of the American Chemical Society, 131 (2009) 10368-10369.

[45] E. Andres-Garcia, L. Oar-Arteta, J. Gascon, F. Kapteijn, ZIF-67 as silver-bullet in adsorptive propane/propylene separation, Chemical Engineering Journal, 360 (2019) 10-14.

[46] P. Krokidas, M. Castier, S. Moncho, D.N. Sredojevic, E.N. Brothers, H.T. Kwon, H.-K. Jeong, J.S. Lee, I.G. Economou, ZIF-67 Framework: A Promising New Candidate for Propylene/Propane Separation. Experimental Data and Molecular Simulations, The Journal of Physical Chemistry C, 120 (2016) 8116-8124.

[47] C. Wang, F. Yang, L. Sheng, J. Yu, K. Yao, L. Zhang, Y. Pan, Zinc-substituted ZIF-67 nanocrystals and polycrystalline membranes for propylene/propane separation, Chemical Communications, 52 (2016) 12578-12581.

[48] H. An, S. Park, H.T. Kwon, H.-K. Jeong, J.S. Lee, A new superior competitor for exceptional propylene/propane separations: ZIF-67 containing mixed matrix membranes, Journal of Membrane Science, 526 (2017) 367-376.

[49] J.R. J. López-Cabrelles, G. Abellán, M. Giménez-Marqués, M. Palomino, S. Valencia, F. Rey, G. Mínguez Espallargas, Solvent-free synthesis of the iron(II) analogue of ZIF-8, Submmitted, under review (2019).

[50] J. Cravillon, S. Münzer, S.-J. Lohmeier, A. Feldhoff, K. Huber, M. Wiebcke, Rapid Room-Temperature Synthesis and Characterization of Nanocrystals of a Prototypical Zeolitic Imidazolate Framework, Chemistry of Materials, 21 (2009) 1410-1412.

[51] C.A. Grande, A.E. Rodrigues, Adsorption of Binary Mixtures of Propane−Propylene in Carbon Molecular Sieve 4A, Industrial & Engineering Chemistry Research, 43 (2004) 8057-8065.

[52] K. Zhou, B. Mousavi, Z. Luo, S. Phatanasri, S. Chaemchuen, F. Verpoort, Characterization and properties of Zn/Co zeolitic imidazolate frameworks vs. ZIF-8 and ZIF-67, Journal of Materials Chemistry A, 5 (2017) 952-957.

[53] C. Zhang, R.P. Lively, K. Zhang, J.R. Johnson, O. Karvan, W.J. Koros, Unexpected Molecular Sieving Properties of Zeolitic Imidazolate Framework-8, The Journal of Physical Chemistry Letters, 3 (2012) 2130-2134.

[54] D.M. Ruthven, R.I. Derrah, K.F. Loughlin, Diffusion of Light Hydrocarbons in 5A Zeolite, Canadian Journal of Chemistry, 51 (1973) 3514-3519.

[55] J. Gascon, W. Blom, A. van Miltenburg, A. Ferreira, R. Berger, F. Kapteijn, Accelerated synthesis of all-silica DD3R and its performance in the separation of propylene/propane mixtures, Microporous and Mesoporous Materials, 115 (2008) 585-593.

[56] Q. Li, A.J. Zaczek, T.M. Korter, J.A. Zeitler, M.T. Ruggiero, Methyl-rotation dynamics in metal-organic frameworks probed with terahertz spectroscopy, Chemical Communications, 54 (2018) 5776-5779.